Theor Chem Acc (2004) 112: 327–334
DOI 10.1007/s00214-004-0592-1

Theoretical
Chemistry Accounts

Regular article

Electrostatic effects in enzyme catalysis: a quantum mechanics/molecular mechanics study of the nucleophilic substitution reaction in haloalkane dehalogenase

Alejandro Soriano[1], Estanislao Silla[1], Iñaki Tuñón[1], Sergio Martí[2], Vicent Moliner[2], Juan Bertrán[3]

[1] Departament de Química Física/IcMol, Universidad de Valencia, 46100, Burjasot, Valencia, Spain
[2] Departament de Ciències Experimentals, Universitat Jaume I, Box 224, 12080 Castellón, Spain
[3] Departament de Química, Universitat Autònoma de Barcelona, 08193, Bellaterra, Barcelona, Spain

Received: 15 September 2003 / Accepted: 18 December 2003 / Published online: 8 June 2004

Abstract. Combined quantum mechanics/molecular mechanics molecular dynamics simulations have been carried out to study the cleavage of the carbon–chlorine bond in 1,2-dichloroethane catalysed by haloalkane dehalogenase from *Xanthobacter Autotrophicus* GJ10. The process has been compared with an adequate counterpart in aqueous solution, the nucleophilic attack of acetate anion on 1,2-dichloroethane. Within the limitations of the model, mainly due to the use of a semiempirical Hamiltonian, our results reproduce the magnitude and characteristics of the catalytic effect. Comparisons of the enzymatic and in solution potentials of mean force reveal that, irrespective of the reference state, the enzyme shows a larger affinity for the transition state. The origin of this increased affinity is found in the differences in the electrostatic pattern created by the environment in aqueous solution and in the enzyme.

Keywords: Enzyme catalysis – Quantum mechanics/molecular mechanics methods – Haloalkane dehalogenase – Potential of mean force – Electrostatic effects

Introduction

Haloalkane dehalogenases are a class of enzymes that catalyses the cleavage of carbon–halogen bonds yielding the corresponding halide anion and an alcohol [1, 2, 3, 4]. These enzymes thus provide a practical way to efficiently remove compounds containing such bonds from the environment, since several of their substrates are potent pollutants. In particular, haloalkane dehalogenase from *Xanthobacter Autotrophicus* GJ10 (DhlA) catalyses the conversion of 1,2-dicloroethane (DCE) to 2-chloroethanol and chloride [5]. X-ray crystal structures for this enzyme at 1.9 Å resolution and for the enzyme–substrate complex at 2.4 Å have been reported [6, 7]. The active site is placed between two domains of the enzyme [4]. The cavity is predominantly formed by hydrophobic residues and the only charged residues close to the active site are Asp124, Asp260 and His289. The complete reaction takes place in two steps [6, 7, 8, 9]. In the first one, DCE undergoes an S_N2 displacement of the chlorine atom by means of the carboxylate group of Asp124, resulting in an ester covalently bound to the enzyme. Trp125 and Trp175 play an essential role in this step by stabilizing the leaving group, the chloride anion, forming hydrogen bonds with it. In a second process, a crystal water molecule, activated by the combined action of His289 and Asp260, hydrolyses the ester (Scheme 1). Thus, the reaction takes place without the use of any aggressive oxidant or metallic ion, which makes it very interesting as a bioremediation technique.

Many computational studies have been devoted to the study of the first reaction step [10, 11, 12, 13, 14, 15, 16, 17, 18, 19, 20, 21, 22] and according to them different explanations about the origin of the catalytic power of DhlA have arisen. In water, the counterpart reaction between DCE and acetate takes place with a free-energy barrier estimated to range between 26 and 29.9 kcal mol^{-1}, while in the enzyme this is reduced to 15.3 kcal mol^{-1} (obtained from Ref. [5] using transition-state (TS) theory applied to k_{cat}). These two values are based on extrapolations from other temperatures [23] or on the use of nucleophilic parameters [21, 22]. This means a catalytic effect between 10.7 and 14.6 kcal mol^{-1}. Following Bruice [20] this enzyme

Proceedings of the 11th International Congress of Quantum Chemistry satellite meeting in honour of Jean-Louis Rivail

Correspondence to: I. Tuñón
e-mail: tunon@uv.es

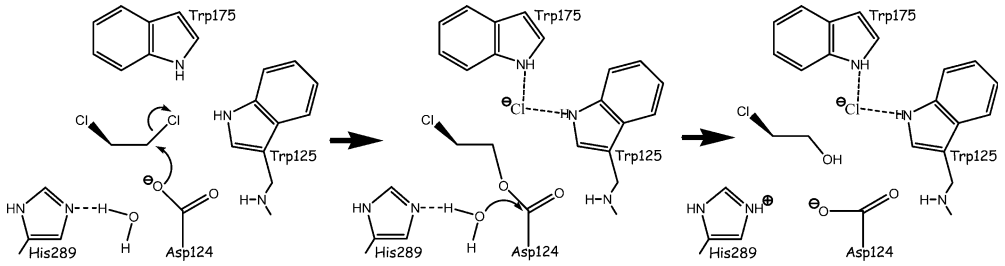

Scheme 1

could compress the reacting fragments (DCE and the carboxylate group of Asp124) in a rearrangement close to the TS structure. This explanation is usually known as the near-attack-conformation (NAC) hypothesis [20, 24] and implies that the enzymes reduce the activation barrier, pushing up the reactants along the reaction path. However, Shurki et al. [22] have quantified this effect and found that its contribution to the total catalytic effect is small (about 2.2 kcal mol^{-1}). According to these authors, enzyme catalysis is the result of TS stabilization relative to water solution caused mainly by electrostatic contributions. In a more recent work Devi-Kesavan and Gao [21] arrived at the conclusion that the catalytic effect is the result of two factors: desolvation of reactants (whose contribution is estimated to be 8 kcal mol^{-1}) and TS electrostatic stabilization.

In a more general perspective, these different proposals are an example of the debate about the origin of enzyme catalysis, a field in which a consensus has not yet been reached. If the reaction mechanism is the same for the uncatalysed and the catalysed reactions, then we can easily relate the difference in their respective activation free energies to the binding energies of the TS and the reactant state (see Scheme 2, where MC represent the Michaelis complex):

$$\Delta G^{\ddagger}_{\mathrm{uncat}} - \Delta G^{\ddagger}_{\mathrm{cat}} = \Delta G^{\mathrm{MC}}_{\mathrm{bind}} - \Delta G^{\mathrm{TS}}_{\mathrm{bind}}.$$

Since the left-hand side of the equation is positive, $\Delta G^{\mathrm{TS}}_{\mathrm{bind}}$ has to be larger, in absolute value, than $\Delta G^{\mathrm{MC}}_{\mathrm{bind}}$. That is, the enzyme presents a larger affinity for the TS than for the reactant state. One could then conclude that enzymes interact better with the TS than with the MC. However, one must realize that these two binding free energies can contain very different contributions. In the case of the TS, the most important geometrical parameters are assumed to remain unchanged when passing from the solution to the enzyme. Thus, $\Delta G^{\mathrm{TS}}_{\mathrm{bind}}$ essentially contains the changes in the interaction energy and the reorganization of the surroundings. However, $\Delta G^{\mathrm{MC}}_{\mathrm{bind}}$ can contain an important energy contribution due to the change in the substrate geometry as far as one usually goes from separated and fully solvated reacting groups in water (in this case the solvated DCE and acetate) to a spatial rearrangement where these are in contact. It can be useful then to consider an imaginary intermediate state in solution (MCS) having the same value of the reaction coordinate that corresponds to the MC in the enzyme. In this way, the binding energy of the reactants ($\Delta G^{\mathrm{MC}}_{\mathrm{bind}}$) can be separated into two terms: the

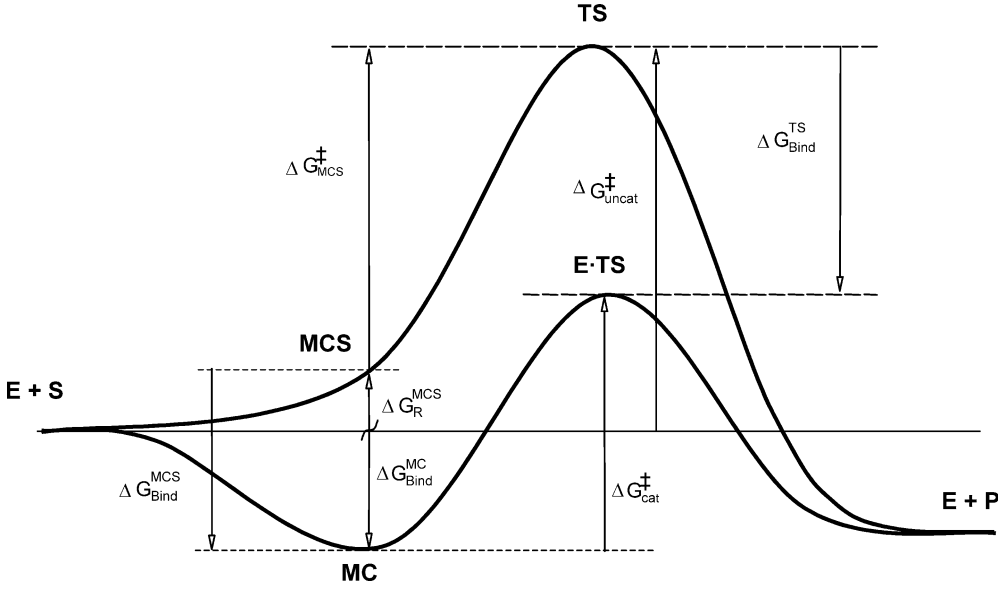

Scheme 2

free energy required in going from the solvent-separated reactants to the MCS (ΔG_R^{MCS}, which is positive by definition) and the binding energy of this structure (ΔG_{bind}^{MCS}). The binding energies of the TS and the MCS can be directly compared as far as the main contribution in both cases is the variation in the interaction energies.

$$\Delta G_{uncat}^{\ddagger} - \Delta G_{cat}^{\ddagger} = \Delta G_R^{MCS} + \Delta G_{bind}^{MCS} - \Delta G_{bind}^{TS}$$

Catalysis can be then obtained in two ways: by means of TS stabilization ($\Delta G_{bind}^{MCS} - \Delta G_{bind}^{TS} > 0$ or by reactant-state destabilization ($\Delta G_R^{MCS} > 0$). Desolvation and NAC production are examples of this last case. The ΔG_R^{MCS} free-energy term can contain either enthalpic or entropic contributions [25, 26, 27, 28].

In this work we present a combined quantum mechanics (QM)/molecular mechanics (MM) statistical study of the S_N2 displacement of the chlorine atom of DCE by a carboxylate group in the active site of DhlA and in aqueous solution. The results are compared with those from previous works and are related to other enzymatic processes, in an attempt to highlight not only this particular enzymatic process but also the more general problem of the origin of enzymatic efficiency speeding up the rate of chemical reactions.

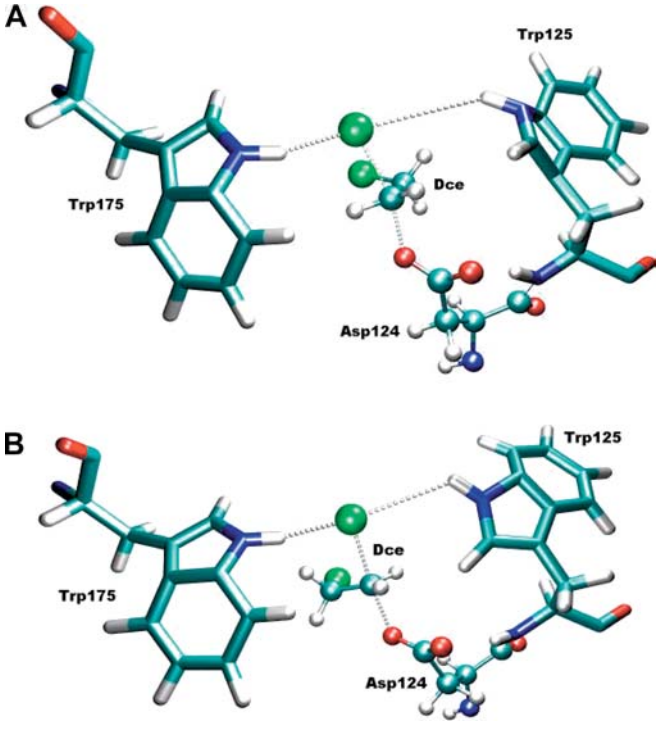

Fig. 1. Snapshots of the transition states (*TSs*) corresponding to the enzymatic path I (**A**) and path II (**B**). Note the different value of the Cl–C–C–Cl dihedral angle

Methodology

A realistic potential-energy function is the first requisite to study a chemical reaction. Because of the size of our systems we used a QM/MM computational scheme where DCE and the side chain of Asp124 are described using QM. In particular we chose the semiempirical parameterized model 3 (PM3) method for our calculations [29]. This Hamiltonian has been previously checked for this same reaction and it provides reasonable results, though systematic overestimation of the activation energy is obtained [17, 21]. The MM subsystem is described by means of the all-atom optimized potential for liquid simulations (OPLS) potential [30] for the enzyme and a flexible TIP3P potential for water molecules [31]. The Lennard-Jones parameters for the QM/MM interaction are also taken from the OPLS potential, except for the QM chlorine atoms, for which we used those of Ref. [32]. These parameters were specifically developed for QM/MM calculations. Although these Lennard-Jones parameters were originally developed for Austin model 1/MM calculations, we tested them with the PM3 Hamiltonian by means of hybrid optimizations of chloride anion–water clusters and obtained results in better agreement with ab initio calculations than with the standard OPLS parameters. The interface between both subsystems was treated using the link-atom methodology [33, 34, 35]. The link atom was placed between the C_A and C_B atoms of Asp124. A switched cutoff radius of 12 Å was employed for all kinds of interactions.

Once the potential-energy surface has been defined we need to explore it to get representative structures of the stationary points of the chemical process. In the case of the enzyme we took the X-ray crystal structure of the enzyme–substrate complex (Protein Data Bank code 2DHC) [6] and placed it in a cavity deleted from a 55.8 Å-side box of TIP3P water molecules. As the resulting system (17,154 atoms in total) was very large we kept frozen all atoms beyond 20 Å from DCE (12,317 atoms). Those atoms are far enough away and a negligible contribution is expected from them. As found in previous work [36] there are two free-energy minima corresponding to the gauche conformers of DCE in the enzymatic active site. From these two minima and employing the GRACE algorithm [37] we located two different transition structures, shown in Fig. 1. These two structures are characterized as true stationary structures having only one imaginary frequency in a coordinate subspace (in this case defined by the coordinates of the QM atoms). To study the counterpart reaction in solution we placed a DCE molecule and an acetate anion in a box of 31.4 Å side of TIP3P water molecules, resulting in 3,081 system atoms (1,022 water molecules). As in the enzyme we located a guess transition structure using GRACE.

Periodic boundary molecular dynamic simulations were performed at 300 K using the *NVT* ensemble with a time step of 1 fs. The integration time step used was

adequate to perform a simulation of this system because during the process no bond involving hydrogen atoms is formed or broken. The umbrella sampling technique was used to compute the potential of mean force (PMF) of the nucleophilic substitution reaction following a distinguished reaction coordinate both in the enzyme and in aqueous solution. Owing to the nature of the reaction we chose as the reaction coordinate the difference between the broken and the formed bonds, i.e., the (C–Cl) distance and the (C–O) distance. Also, to overcome the energy barrier, we added a biased potential to this reaction coordinate. The value of the force constant used for the umbrella sampling (3,000 kJ mol^{-1} $Å^{-2}$) was determined to allow full overlapping of the different windows traced in the PMF evaluation. The probability distributions, obtained from each individual window, were put together by means of the weighted histogram analysis method (WHAM) [38]. The length of each window (10 ps) and the total number of windows (80) proved to be long enough to sample a wide range of structures at the reference temperature. For these values, the step used in the reaction coordinate was 0.0375 Å.

To obtain the respective PMF of the reaction in aqueous solution we kept frozen the relative orientation of the two reacting fragments (acetate and DCE), avoiding in this way the sampling of irrelevant structures. This restriction was unnecessary when obtaining the enzymatic PMFs since the environment already imposed an adequate orientation of the fragments. To get the full PMF in aqueous solution we estimated the free energy of releasing the restrictions imposed on our system following the method in Ref. [39]. We calculated this contribution for several values of the reaction coordinate and after interpolation it was added to the restricted PMF to obtain the full PMF for the S_N2 displacement in water solution.

The properties of the TS and the reactant state were obtained from longer simulations carried out at the windows placed at the maximum and minimum of the PMFs, respectively.

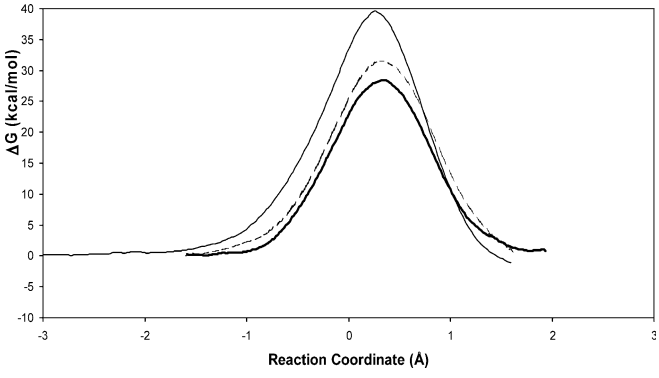

Fig. 2. Potentials of mean force obtained for the reaction in the enzyme (path I *dashed line*, path II *bold line*) and in aqueous solution (*normal line*)

Results and discussion

Potentials of mean force

As we showed in previous work [36], when the substrate binds to DhlA, two possible free-energy minima, corresponding to the nonequivalent gauche conformations of DCE, are found. The conformational equilibrium of DCE is determined by electrostatic interactions and the free-energy difference between the two minima is quite small (0.3 kcal mol^{-1}). For this reason we investigated the two possible reaction channels. Starting from the two gauche conformers we obtained two different transition structures (Fig. 1) from which the corresponding PMFs (I and II) were traced. These PMFs are shown in Fig. 2. The activation free energy obtained from path II is somewhat lower than from path I (28.4 versus 31.5 kcal mol^{-1}). Averaged geometrical parameters corresponding to the TS and the reactant state of both enzymatic paths are given in Table 1. The difference between the activation free energies of the two enzymatic paths (3.1 kcal mol^{-1}) is in agreement with the estimations of Bruice [20] based on potential-energy-surface exploration. The PMF for the reaction between acetate anion and DCE in aqueous solution is also shown in Fig. 2.

The activation free energies are summarized in Table 2 and are compared with the experimental values. As expected, the PM3/MM calculations severely overestimate the activation free energies, but the catalytic effect, which is the difference between the activation free energies in the enzyme and in solution, is quite well reproduced in our calculations. The expected error of

Table 1. Selected average geometrical parameters (distances in angstroms and angles in degrees) for the reactant states (*RS*) and transition states (*TS*) of the enzymatic reaction

	Path I		Path II	
	RS	TS	RS	TS
$Asp124O^{\delta 2}$–C	3.22	1.94	3.20	1.94
C–Cl	1.82	2.26	1.81	2.27
Reaction coordinate	−1.40	0.32	−1.39	0.33
$Asp124O^{\delta 2}$–C–Cl	158	171	146	168
Cl–C–C–Cl	−82	−92	84	86
$Trp125H^{\epsilon 1}$–Cl	3.37	3.12	3.61	3.37
$Trp175H^{\epsilon 1}$–Cl	4.58	2.51	3.06	2.53

Table 2. Calculated and experimental activation free energies (kcal mol^{-1})

		$\Delta G^{\ddagger}$ (PM3/MM)	$\Delta G^{\ddagger}_{corr}$	Expt.
Enzyme	Path I	31.5		
	Path II	28.4	16.6	15.3
Solution		39.6	30.0	26,29.9[a]
$\Delta\Delta G^{\ddagger}$		11.2	13.4	10.7–14.6

[a]See Refs. [21, 22, 23]

the PM3 Hamiltonian as compared with G2 calculations for the acetate plus DCE reaction in the gas phase is 9 kcal mol^{-1} [21]. As an attempt to correct this error we evaluated a correction term as the difference between the in vacuo energy barrier calculated at the MP2/6-31 + G* level and the PM3 one, but using the averaged geometries of the reactant state and the TS in the enzyme and in solution. The corrected values, $\Delta G^{\ddagger}_{corr}$, are also listed in Table 2. Then, our best estimations for the catalysed and uncatalysed activation free energies would be 16.6 and 30.0 kcal mol^{-1}, respectively, in good agreement with experiment. It is also interesting to compare our results with the recent calculations of Devi-Kesavan and Gao [21]. In that work the authors obtained a PM3/MM free-energy barrier of 23.0 kcal mol^{-1}, which is 5.4 kcal mol^{-1} below our PM3 estimation. The difference is probably due to the fact that in our reactant state the chlorine atom interacts better with the H$^{\epsilon}$ of Trp125 and Trp175 and thus it is more stabilized. The average values provided in Ref. [21] for these two hydrogen bonds are 4.3 and 3.7 Å in the reactant state, to be compared with 3.6 and 3.1 Å in our case (reactant state of path II in Table 1). The average distances in the TSs are more similar (3.3 and 2.6 Å in Ref. [21], compared with 3.4 and 2.5 Å in this work). The use of different Lennard-Jones parameters for the chlorine atom could explain partly this discrepancy. With respect to the reaction free energy, our enzymatic PMF shows a nearly thermoneutral process. For this quantity, the error associated with the use of the semiempirical PM3 Hamiltonian is expected to be small (about 0.6 kcal mol^{-1} in the gas phase when compared with G2 calculations [21]). In contrast, the results of Devi-Kesavan and Gao [21] show an exergonic process, with the products being 16 kcal mol^{-1} stabler than the reactants. A recent kinetic isotopic analysis [14] indicates that the nucleophilic step of the global reaction is most probably reversible and thus our calculations would reproduce better this experimental finding.

Single mutations of the two tryptophans to glutamine showed a decreased catalytic efficiency and binding constant [8, 40]. Interestingly, mutation of Trp175 has a larger effect on these two magnitudes. This is in agreement with the shorter hydrogen-bond distances observed between the chlorine atom and the H$^{\epsilon}$ of Trp175 in the reactant state and the TS for enzymatic path II, the one presenting a lower activation free energy

Origin of catalysis: analysis of electrostatic effects

To get deeper insight into the origin of the enzymatic efficiency to catalyse a chemical reaction, we must compare it with an adequate counterpart process in aqueous solution. In this case we modelled the uncatalysed reaction in aqueous solution as a nucleophilic attack of acetate anion on DCE. The corresponding PMF is also presented in Fig. 2. Compared with the enzymatic PMF we can point out two significant differences. The first one is that the uncatalysed reaction, as expected, displays a larger activation free energy (39.6 kcal mol^{-1} at the PM3 level and 30.0 kcal mol^{-1} when corrected) than any of the enzymatic paths. Secondly, as discussed in the Introduction, while the TS appears at a value of the reaction coordinate similar to the enzymatic paths (0.29 versus 0.33 Å), the reactant state now corresponds to the fully separated and solvated acetate anion plus DCE (with a reaction coordinate of minus infinity).

As already discussed, our PMF calculations, within the limitations of the model, give a reasonable picture of the process studied in good agreement with the experimental findings, especially the free-energy-barrier lowering caused by the enzyme. Following the analysis presented in the Introduction the direct comparison of the activation free energies for the catalysed and the uncatalysed processes can be related to the difference in the binding free energies of the TS and the reactant state

$$\Delta G^{\ddagger}_{uncat} - \Delta G^{\ddagger}_{cat} = \Delta G^{MCS}_{bind} - \Delta G^{TS}_{bind} = 11.2 \text{ kcal mol}^{-1}$$

using the PM3/MM values. However, as discussed previously, this difference cannot be directly interpreted as the preferential interaction of the enzyme with the TS charge distribution. Indeed, the binding energies of the TS and the reactant state can contain different contributions. In our case, the aqueous solution TS appears at a value of the reaction coordinate (0.29 Å) very similar to that found for the enzymatic reaction (0.33 Å). However, while the reactant state in the enzyme (the MC) appears at −1.39 Å, the free-energy minimum in solution is found when the distance between the acetate anion and DCE is infinite. From our aqueous solution PMF we can easily estimate the free energy needed to make the reacting fragments reach the value of the reaction coordinate corresponding to the MC, i.e. ΔG^{MCS}_{R}. The value obtained is 1.7 kcal mol^{-1}, in good agreement with the estimation of Shurki et al. [22] of about 2.2 kcal mol^{-1}. It must be pointed out that this quantity was obtained in solution. Gas-phase calculations of the energy needed to rearrange the reactant fragments into a structure similar to the MC are not relevant in our thermodynamic scheme and can lead to erroneous interpretations [41]. It could be argued that formation of the MC also involves changes in other relevant coordinates and then our calculation would only be a lower limit. However, comparison of the MC and MCS dynamics does not reveal seemingly important differences. In any case contributions from other degrees of freedom to the binding free energy can be expected to be smaller [22] and to cancel out, at least partly, as they can be similar in the TS and the MCS. Once ΔG^{MCS}_{R} has been obtained we can now compare the binding energies of the TS and of the MCS. These binding energies are expected to contain similar contributions because the energy needed to rearrange the reactants along the reaction coordinate has been removed:

$$\Delta G^{\ddagger}_{\mathrm{MCS}} - \Delta G^{\ddagger}_{\mathrm{cat}} = \Delta G^{\mathrm{MCS}}_{\mathrm{bind}} - \Delta G^{\mathrm{TS}}_{\mathrm{bind}} = 9.5 \text{ kcal mol}^{-1}.$$

Thus, the enzyme clearly presents a larger affinity for the TS irrespective of our reference state (the reactant state or the MCS). The real question concerning enzyme catalysis is how the differential binding is achieved by the enzyme relative to a proper reference state in aqueous solution. We then decided to investigate the different electrostatic patterns created by the enzymatic and the aqueous MM environments. The modulus of the electric field created by the aqueous environment on the nucleophilic oxygen of the acetate anion and on the attacked carbon atom of DCE during a simulation of the MCS is displayed in Fig. 3a. In aqueous solution, the electric field created by the solvent molecules is a reaction field, dominated by the negative charge of the acetate plus DCE system. We have a strong field with a very similar value on the two atoms (the average modulus is 0.0121 and 0.0126 a.u. on the carbon and oxygen atoms). The same electric field during a simulation of the MC of path II in the enzyme active site is shown in Fig. 3b. Now, the electric field on the oxygen atom is very similar to what we found in water, with an average

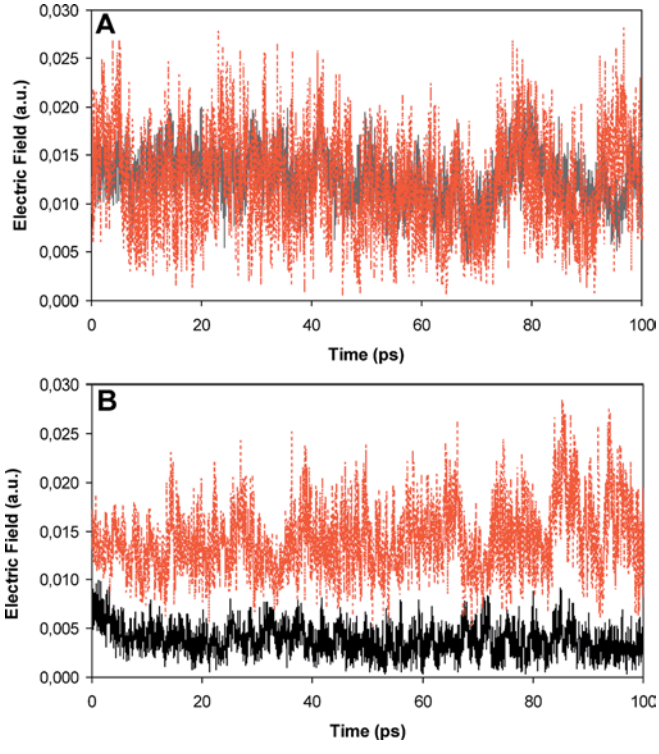

Fig. 3. Average modulus of the electric field created by the molecular mechanics (*MM*) environment on the nucleophilic oxygen (*red line*) and on the attacked carbon atom (*black line*) for **A** the Michaelis complex intermediate state (*MCS*) in solution and for **B** the Michaelis complex (*MC*) of path II in the enzyme

modulus of about 0.0142 a.u. Then, from an electrostatic point of view we did not find significant desolvation of the nucleophilic oxygen atom in the enzyme active site. Although not shown here, the same is true for the leaving chlorine atoms, with the average electric field on these atoms being 0.0071 and 0.0074 a.u. in aqueous solution and in the enzyme, respectively. What is really different in both media is the electric field on the carbon atom. In the enzyme this electric field is much lower than in water, with an average value of only 0.0038 a.u. Moreover, this electric field is not only different in magnitude but also in orientation. In water, the electric field on the carbon atom is essentially oriented along the line that joins the nucleophilic oxygen and the leaving chloride anion, i.e. the direction of the nucleophilic attack. The average component along this line is 0.0102 a.u. This component of the field acts as a force hindering the conversion of the reactants towards the TS-like configuration [$O^{\delta-}$–$C^{\delta+}$–$Cl^{\delta-}$], as also found for other similar S_N2 reactions in solution [42]. In the enzyme the projection of the electric field on this line averages to zero and then this force vanishes.

From the aforementioned results, we can conclude that electrostatic effects in the enzyme can be as important as in water solution, but they have some key differences. First, the enzymatic electric field presents large changes in magnitude when going from the nucleophilic oxygen atom to the carbon atom in the MC. This is obviously related to the more heterogeneous composition of the enzyme active site with respect to the solvent cage where the MCS is placed. The existence of hydrophobic, nonpolar, residues in the enzyme active site is clearly related to this characteristic and it could be indispensable to modulate such an electric field. Second, the solvent electric field is a reaction field whose magnitude and orientation is determined by the solvent response to the solute electric properties. This has very important consequences for the energetics of the reaction. The TS of a nucleophilic substitution that goes from charged reactants to charged products is less polar than the reactant state and thus is less stabilized by the solvent reaction field. The consequence is that solvent effects increase the activation energy of the reaction, as can be deduced from the Hughes–Ingold rules [43]. However, that is not necessarily true if the environmental electric field is not a reaction field, as in the case of the enzyme.

From an electronic point of view the S_N2 reaction can be seen as the transfer of a negative charge from the nucleophilic oxygen atom (the donor) to the leaving chloride anion (the acceptor). The question is how the environment within which the reaction occurs affects the energetics of this transfer of charge. To answer this, we evaluated the average electrostatic potential along the vector connecting the donor O and the acceptor Cl atoms, due to the charge distribution of the MM environment, in the trajectories corresponding to the MC and the TS for both water and enzyme (path II)

environments. A plot of the variation of the electrostatic potential created by water or the enzyme at positions along the line of the nucleophilic attack (the O–Cl vector) is shown in Fig. 4. A value $d=0$ indicates the position of the nucleophilic oxygen and a value $d=1$ corresponds to the position of the chlorine atom. A negative value of the electrostatic potential indicates a repulsive interaction between the negative charge and the MM environment, whereas a positive value indicates an attractive interaction. Inspection of the "MCS water" curve shows a decreasing potential from the oxygen atom to chlorine. This means that the potential is substantially more positive on the oxygen atom than on the chlorine atom. Then, the MM environment of the solvent water molecules is well suited for stabilization of the charge distribution of the reactants, but is badly matched to the product complex. According to this, we must do extra work to transfer the negative charge against the solvent electrostatic potential, which can be evaluated as $W=\Delta q\cdot\delta V$. In the TS the charge is already partly transferred from the oxygen to the chlorine atom and then the "TS water" curve corresponds to a solvent distribution complementary to this new situation. Obviously, the change in the solute charge distribution implies a significant rearrangement of the solvent molecules, which is here reflected in the very different electrostatic potential arising in both states.

The curve for "MC enzyme" shows again a more positive electrostatic potential on the oxygen atom than on the chlorine atom, indicating that when the environment is in equilibrium with the MC extra work must be done to complete the reaction from the electronic point of view. However, the variation of the electrostatic potential is now much smaller than in solution, 0.14 versus 0.23 a.u. Then the work needed to complete the transfer of charge in this environment is lower than that in solution. Moreover, the curves corresponding to the MC and the TS in the enzyme are very similar. The electrostatic potential difference between the MC and the TS is much smaller in the enzyme active site than in water. The electrostatic field created by the enzyme is mainly due to a permanent charge distribution and thus it remains essentially unaltered, and in a favourable orientation, relative to water, during the progress of the reaction. In contrast, the reaction field in water reflects the polarization of the solvent induced by the solute polarity.

The electrostatic potential is also a useful tool to analyse the role played by different residues or groups of residues on the reaction. For example, the two tryptophans, Trp125 and Trp175, are expected to favour the reaction progress stabilizing the leaving group by means of hydrogen bonds between the chlorine atom and the polar H^{ϵ} atoms. The contribution of the two tryptophans to the enzymatic electrostatic potential averaged during simulations corresponding to the MC for paths I and II is displayed in Fig. 5. In both cases these residues create a positive potential along the vector joining the donor and acceptor atoms. However, only in the case of path II is the electrostatic potential due to these residues more positive on the chlorine atom than on the oxygen atoms and then only in this case are they correctly oriented in the MC for the stabilization of the charge transfer taking place during the progress of the reaction.

Conclusions

In this work we have presented a combined QM/MM molecular dynamics study of the first step of the enzymatic conversion of 1,2 dichloroethane to 2-chloroethanol and chloride anion. The results agree reasonably with experience considering the limitations of the semiempirical PM3 Hamiltonian employed in our

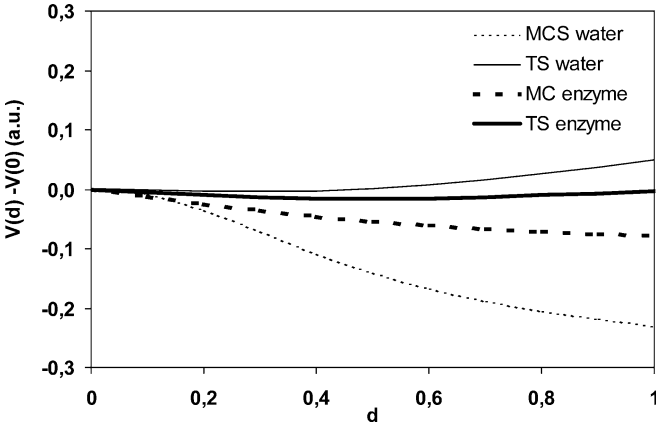

Fig. 4. Variation of the average electrostatic potential created by the MM environment along the vector joining the nucleophilic oxygen and the leaving chlorine atoms for the MCS and the TS in solution and for the MC and the TS of the enzymatic path II. Note that the O–Cl distance has been normalized to average the different structures appearing during the simulation

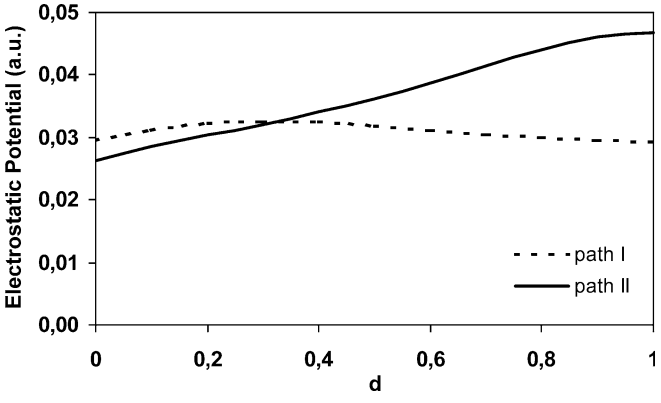

Fig. 5. Average contribution of Trp125 and Trp175 to the electrostatic potential calculated along the vector joining the the nucleophilic oxygen and the leaving chlorine atoms for the MC of paths I and II

treatment. In order to highlight the origin of the enzyme ability to speed up the chemical rate of this process we compared the results with those of the nucleophilic attack of acetate anion on DCE in aqueous solution. The difference between the activation free energies of the catalysed and the uncatalysed processes can be related to the difference between the binding energies of the TS and the reactant state. The problem is that in this case this direct comparison can be inconclusive about the magnitude of the substrate–enzyme interactions in each state as far as the reactant states in the enzyme and in solution are quite different. In such a case the binding energies can contain substantial contributions due to the rearrangement of the reactants. For this reason we introduced a MC-like complex in solution, even if it is not a real free-energy minimum, defined as the reactant state appearing along the PMF having the same value of the reaction coordinate as the MC. From our PMFs it can be easily deduced that irrespective of the reference state taken for the in solution process (reactant state or MCS) the enzyme shows increased affinity for the reaction TS:

$$\Delta G_{\text{bind}}^{\text{MC}} - \Delta G_{\text{bind}}^{\text{TS}} \geqslant \Delta G_{\text{bind}}^{\text{MC}} - \Delta G_{\text{bind}}^{\text{TS}} > 0.$$

This relationship means that the main role played by the enzyme is just to stabilize the TS more than the reactant state (or MCS) relative to the process in solution. We then looked for the origin of this relative stabilization by studying the different electrostatic effects caused by the two media: the solvent and the enzyme. In solution we have a reaction field dominated by the negative charge of the solute. When the reaction proceeds, from the reactant state to the TS, the polarity of the solute diminishes, which in turn provokes a diminution of the solvent reaction field. As a consequence, the TS is less stabilized by electrostatic interactions than the reactant state and the final effect is a net increase of the activation free energy. In the enzyme we have an electric field presenting significant differences with respect to the solvent. In the case of the enzyme the surroundings oppose less the changes taking place in the substrate charge distribution during the progress of the reaction. The enzyme electric field is not a reaction field and then it does not necessarily diminish when the substrate polarity does. The reaction field in solution is in equilibrium with the solute charge distribution, whereas in the enzyme it has a large permanent part. We can then conclude that the structure of the enzyme is designed to electrostatically favour the TS relative to the reactant compared with the process in solution.

Acknowledgements. We are indebted to DGI for project BQU2000-C03 and Generalitat Valenciana for project GV01-324, which supported this research. A.S. thanks the Universitat de València for a doctoral "V Segles" fellowship. S.M. thanks the UJI-BANCAIXA Foundation for a postdoctoral fellowship.

References

1. Janssen DB, Scheper A, Dijkhuizen L, Witholt B (1985) Appl Environ Microbiol 49:673
2. Wischnak C, Muller R (2000) Biotechnology 11b:241
3. Ridder IS, Dijkstra BW (2000) Cattech 3:126
4. Franken SM, Rozeboom HJ, Kalk KH, Dijkstra BW (1991) EMBO J 10:1297
5. Schanstra JP, Kingma J, Janssen DB (1996) J Biol Chem 271:14747
6. Verschueren KH, Seljee F, Rozeboom HJ, Kalk KH, Dijkstra BW (1993) Nature 363:693
7. Verschueren KH, Franken SM, Rozeboom HJ, Kalk KH, Dijkstra BW (1993) J Mol Biol 232:856
8. Kennes C, Pries F, Krooshof GH, Bokma E, Kingma J, Janssen DJ (1995) Eur J Biochem 228:403
9. Pries F, Kingma J, Krooshof GH, Jeronimus-Stratingh CM, Bruins AP, Janssen DB (1995) J Mol Biol 18:10405
10. Damborsky J, Kuty M, Nemec M, Koca J (1997) J Chem Inf Comput Sci 37:562
11. Damborsky J, Bohac M, Prokop M, Kuty M, Koca J (1998) Protein Eng 11:901
12. Damborsky J, Koca J (1999) Protein Eng 12:989
13. Kuty M, Damborsky J, Prokop M, Koca J (1998) J Chem Inf Comput Sci 38:736
14. Lewandowicz A, Rudzinski J, Tronstad L, Widersten M, Ryberg P, Matsson O, Paneth P (2001) J Am Chem Soc 123:4550
15. Lightstone FC, Zheng YJ, Bruice TC (1998) Bioorg Chem 26:169
16. Lightstone FC, Zheng YJ, Bruice TC (1998) J Am Chem Soc 120:5611
17. Maulitz AH, Lightstone FC, Zheng YJ, Bruice TC (1997) Proc Natl Acad Sci USA 94:6591
18. Lau EY, Kahn K, Bash PA, Bruice TC (2000) Proc Natl Acad Sci USA 97:9937
19. Lightstone FC, Bruice TC (1999) Acc Chem Res 32:127
20. Bruice TC (2002) Acc Chem Res 35:139
21. Devi-Kesavan LS, Gao J (2003) J Am Chem Soc 125:1532
22. Shurki A, Strajbl M, Villà J, Warshel A (2002) J Am Chem Soc 124:4097
23. Okamoto K, Kita T, Araki K, Shingu H (1967) Bull Chem Soc Jpn 40:1912
24. Benkovic SJ, Bruice TC (2000) Biochemistry 39:6267
25. Page MI, Jenks WP (1971) Proc Natl Acad Sci USA 68:1678
26. Villà J, Strajbl M, Glennon TM, Sham YY, Chu ZT, Warshel A (2000) Proc Natl Acad Sci USA 97:11899
27. Menger FM (1999) J Am Chem Soc 1121:11831
28. Kollman PA, Kuhn B, Donini O, Peräkylä M, Stanton RV, Bakowies D (2001) Acc Chem Res 34:72
29. Stewart JJP (1989) J Comput Chem 10:209
30. Jorgensen WL, Maxwell DS, Tirado-Rives J (1996) J Am Chem Soc 118:11225
31. Jorgensen WL, Chandrasekhar J, Madura JD, Impey RW, Klein ML (1983) J Chem Phys 79:926
32. Gao J, Xia X (1993) J Am Chem Soc 115:9667
33. Reuter N, Dejaegere A, Maigret V, Karplus M (2000) J Phys Chem A 104:1720
34. Singh H, Kollman P (1986) J Comput Chem 7:718
35. Field M, Bash PA, Karplus M (1990) J Comput Chem 11:700
36. Soriano A, Silla E, Tuñón I (2003) J Phys Chem B 107:6234
37. Moliner V, Turner AJ, Williams IH (1997) J Chem Soc Chem Commun 1271
38. Valleau J P, Torrie G M (1977) J Comput Phys 23:187
39. Hermans J, Wang L (1997) J Am Chem Soc 119:2707
40. Krooshof GH, Ridder IS, Tepper AWJW, Vos GJ, Rozeboom HJ, Kalk KH, Dijkstra BW, Janssen DB (1998) Biochemistry 37:15013
41. Strajbl M, Shurki A, Kato M, Warshel A (2003) J Am Chem Soc 125:10228
42. Gertner BJ, Whitnell RM, Wilson KR, Hynes JT (1991) J Am Chem Soc 113:74
43. Hughes ED, Ingold CK (1935) J Chem Soc 244:252